Diuretic drug binding to human glutathione transferase P1-1: Potential role of Cys-101 revealed in the double mutant C47S/Y108V

ARTICLE *in* JOURNAL OF MOLECULAR RECOGNITION · MARCH 2011

Impact Factor: 2.15 · DOI: 10.1002/jmr.1040 · Source: PubMed

Research Article

Journal of Molecular Recognition

Received: 6 December 2009, Revised: 26 February 2010, Accepted: 15 March 2010, Published online in Wiley Online Library: 10 June 2010

(wileyonlinelibrary.com) DOI:10.1002/jmr.1040

Diuretic drug binding to human glutathione transferase P1-1: potential role of Cys-101 revealed in the double mutant C47S/Y108V

Indalecio Quesada-Soriano[a,†], Lorien J. Parker[b,c,†], Alessandra Primavera[d,†], Jerome Wielens[b], Jessica K. Holien[b], Juan M. Casas-Solvas[e], Antonio Vargas-Berenguel[e], Ana M. Aguilera[a], Marzia Nuccetelli[f], Anna P. Mazzetti[d], Mario Lo Bello[d], Michael W. Parker[b,c] and Luis García-Fuentes[a]*

The diuretic drug ethacrynic acid (EA), both an inhibitor and substrate of pi class glutathione S-transferase (GST P1-1), has been tested in clinical trials as an adjuvant in chemotherapy. We recently studied the role of the active site residue Tyr-108 in binding EA to the enzyme and found that the analysis was complicated by covalent binding of this drug to the highly reactive Cys-47. Previous attempts to eliminate this binding by chemical modification yielded ambiguous results and therefore we decided here to produce a double mutant C47S/Y108V by site directed mutagenesis and further expression in *Escherichia coli* and the interaction of EA and its GSH conjugate (EASG) examined by calorimetric studies and X-ray diffraction. Surprisingly, in the absence of Cys-47, Cys-101 (located at the dimer interface) becomes a target for modification by EA, albeit at a lower conjugation rate than Cys-47. The Cys-47 → Ser mutation in the double mutant enzyme induces a positive cooperativity between the two subunits when ligands with affinity to G-site bind to enzyme. However, this mutation does not seem to affect the thermodynamic properties of ligand binding to the electrophilic binding site (H-site) and the thermal or chemical stability of this double mutant does not significantly affect the unfolding mechanism in either the absence or presence of ligand. Crystal structures of apo and an EASG complex are essentially identical with a few exceptions in the H-site and in the water network at the dimer interface.

Keywords: calorimetry; protein-ligand interaction; crystallography; binding; ethacrynic acid; glutathione transferase; kinetic studies; docking studies; thermodynamic

INTRODUCTION

The glutathione transferases (EC 2.5.1.18) (GSTs) are a family of enzymes involved in cellular detoxification. They catalyse the nucleophilic attack of glutathione (GSH) on the electrophilic centre of a number of toxic compounds and xenobiotics (Hayes *et al*., 2005). The cytosolic members of the family have been grouped into at least seven species-independent classes: alpha, mu, pi, theta, sigma, zeta and omega (Mannervik *et al*., 2005), on the basis of N-terminal sequence, substrate specificity and immunological properties (Meyer *et al*., 1991). Their three-dimensional folds do not differ significantly despite a low level of sequence homology. Each subunit contains a very similar binding site for GSH (G-site) and a second binding site for

* *Correspondence to: L. García-Fuentes, Department of Physical Chemistry, Faculty of Experimental Sciences, University of Almería, La Cañada de San Urbano, 04120 Almería, Spain.*
E-mail: lgarcia@ual.es

a *I. Quesada-Soriano, A. M. Aguilera, L. García-Fuentes*
Department of Physical Chemistry, Faculty of Experimental Sciences, University of Almería, La Cañada de San Urbano, 04120 Almería, Spain

b *L. J. Parker, J. Wielens, J. K. Holien, M. W. Parker*
Biota Structural Biology Laboratory, St. Vincent's Institute of Medical Research, Fitzroy, Victoria 3065, Australia

c *L. J. Parker, M. W. Parker*
Department of Biochemistry and Molecular Biology, Bio21 Molecular Science and Biotechnology Institute, The University of Melbourne, Parkville, Victoria 3010, Australia

d *A. Primavera, A. P. Mazzetti, M. L. Bello*
Department of Biology, University of Rome 'Tor Vergata', 00133 Rome, Italy

e *J. M. Casas-Solvas, A. Vargas-Berenguel*
Department of Organic Chemistry, Faculty of Experimental Sciences, University of Almería, La Cañada de San Urbano, 04120 Almería, Spain

f *M. Nuccetelli*
Department of Laboratory Medicine, University of Rome 'Tor Vergata', 00133 Rome, Italy

† *These authors have contributed equally to this work.*

Abbreviations used: *DSC, differential scanning calorimetry; DTT, dithiothreitol; EA, ethacrynic acid; EACys, ethacrynic-cysteine conjugate; EAME, ethacrynic-mercaptoethanol conjugate; EASG, ethacrynic-glutathione conjugate; GSNO, S-nitrosoglutathione; GST, glutathione S-transferase; GST P1-1, human glutathione transferase P1-1; HEPES, N-(2-hydroxyethyl)-piperazine-N'-2-ethanesulfonic acid; ITC, isothermal titration calorimetry; MES, 2-morpholinoethanesulfonic acid; MPD, 2-methyl-2,4-pentanediol; PEG, polyethylene glycol; wt, wild type.*

the hydrophobic co-substrate (H-site). Structural differences in the H-site confer a certain degree of substrate selectivity (Wilce and Parker, 1994).

Class pi glutathione transferase (GST P1-1), a homodimeric protein of ~46 kDa, has been extensively studied because of the clinical interest in it as a potential marker during chemical carcinogenesis (Tsuchida *et al*., 1989; Townsend *et al*., 2005) and its potential role in the mechanism of cellular multi-drug resistance against a number of anti-neoplastic agents (Black *et al*., 1990). Ethacrynic acid (EA, [2,3-dichloro-4-(2-methylenebutanoyl)-phenoxy] acetic acid) is a potent diuretic drug that has been used as a therapeutic agent for several decades. Unfortunately, due to unwanted toxic side effects, EA was withdrawn and replaced with furosemide, a diuretic with fewer side effects (Kim *et al*., 1971). EA, an effective inhibitor of GST P1-1, has also been investigated as a potential anti-cancer drug (Lo and Ali-Osman, 2007). In addition to being an inhibitor, EA can also act as a substrate, forming a conjugate with GSH via Michael addition (EASG), both spontaneously and by GST-driven catalysis, by pi, mu and alpha class GSTs (Ploemen *et al*., 1990; Phillips and Mantle, 1991; Awasthi *et al*., 1993). Recently, we investigated the role of a catalytically important residue located in the H-site, Tyr-108, in binding and catalysis of a range of GST P1-1 ligands including EA (Lo Bello *et al*., 1997; Nuccetelli *et al*., 1998; Quesada-Soriano *et al*., 2009). These studies highlighted the importance of Tyr-108: both the hydroxyl and aromatic moieties were found to be involved in the stabilization of certain ligands with changes to this residue by mutation adversely affecting ligand binding to the H-site.

Other important residues thought to be involved in the stabilization and interactions of certain ligands are the cysteine residues of GST P1-1. The pi isoenzymes from four different species have three highly conserved cysteines (Cys-14, Cys-47 and Cys-169). A fourth cysteine (Cys-101) is conserved in all but the mouse isoenzyme (Hatayama *et al*., 1990). The function of the cysteinyl residues has been widely investigated (Ricci *et al*., 1991; Tamai *et al*., 1991; Lo Bello *et al*., 1995, 2001; Vega *et al*., 1998). Cysteine residues have been implicated in the catalytic activity of pi-class GSTs by a number of groups based on the observation that thiol-reactive agents cause inhibition (Ricci *et al*., 1991; Lo Bello *et al*., 1990; Tamai *et al*., 1990). However, the pi-class crystal structures showed that there are no cysteines in either the G- or H-sites (Reinemer *et al*., 1992). Furthermore, site-directed mutagenesis of the cysteines showed they were not directly involved in catalysis (Tamai *et al*., 1991; Nishihira *et al*., 1992). Chemical modification of GST P1-1 showed that modification of Cys-47 was responsible for enzyme inhibition and that the enzyme was only inhibited by certain thiol-reactive reagents such as N-ethylmaleimide (Tamai *et al*., 1991; Nishihira *et al*., 1992). Cys-47 is located in a highly flexible helix-loop region, termed the α2 loop, which is located on the surface of the N-terminal domain with its thiol group pointing into a small hydrophobic pocket contributed by the main chain atoms of Lys-44 and Gln-51 and the side chain atoms of Trp-38 and Leu-52. In GST P1-1, it has a pK_a value of 4.2 and may exist as an ion pair with the protonated ε-amino group of Lys-54 under physiological conditions (Lo Bello *et al*., 1993). The opposite face of this wall comprises part of the G-site. Chemical modification or mutation of Cys-47 would disturb the structure of the inner wall leading to the repositioning of key residues that recognize and bind GSH. Nevertheless, structural studies show the binding site is about 10 Å away from Cys-47 (Reinemer *et al*., 1992). In the oxidized form of GST P1-1, Cys-101 (located at the dimer interface) can form a disulfide bridge with Cys-47 (Ricci *et al*., 1991). These cysteines are 18.8 Å apart in the crystal structure of the reduced enzyme suggesting that α2 loop might encroach into the H-site for the disulfide to form. Molecular dynamic studies have led to the hypothesis that the α2 loop might normally sit in the substrate binding site in the unliganded state because, unlike the other GST classes, the substrate binding site is more exposed and it would be energetically more favourable to bury its hydrophobic surface from the aqueous environment (Wilce and Parker, 1994). The loop is not observed at all in crystal structures of the apo form of the wt enzyme, presumably because of high mobility (Oakley *et al*., 1998).

In order to thoroughly investigate the effect of the Y108V mutation on the intrinsic binding of EA to GST P1-1 it is essential to prevent the chemical modification of Cys-47 by EA that has been shown to occur (Ploemen *et al*., 1990, 1994; Quesada-Soriano *et al*., 2009). In our previous work we explored methods that would allow us to prevent the covalent modification of Cys-47: by chemical modification with alkylating agents, by protection with methylSG or by modifications of the EA inhibitor itself (using EACys and EAME conjugates) (Quesada-Soriano *et al*., 2009). However, these procedures proved insufficient to avoid the chemical modification of the enzyme by EA and consequently prevented further investigation into the effect of Y108V mutation on the intrinsic binding of this drug to GST P1-1.

Here we designed a GST P1-1 double mutant, C47S/Y108V, to remove the potential EA target site, Cys-47, that causes the irreversible modification of the enzyme. We constructed and expressed, in *E. coli*, the double mutant and its kinetic, thermodynamic and structural properties have been studied in detail. Surprisingly, this double mutation does not remove the covalent modification of the enzyme by EA. We conclude that when Cys-47 is mutated, Cys-101 can act as target for modification by EA. Hence, in addition to binding in the active site, Cys-101 might also be a potential target for EA binding.

MATERIALS AND METHODS

Materials

GSH, 1-chloro-2, 4-dinitrobenzene (CDNB), S-hexylglutathione (hexylSG) and EA, NBD-Cl (7-chloro-4-nitrobenz-2-oxa-1, 3-diazole) were purchased from Sigma. EASG and EACys (EA conjugate with L-cysteine) were synthesized and their purity analysed as described previously (Quesada-Soriano *et al*., 2009). Other chemicals employed were of the highest available purity.

Activation parameters determination

The temperature dependence of the kinetic constants for chemical conjugation was analysed according to transition state theory (Fersht, 1999). Thermodynamic activation parameters, $\Delta G^{\neq}$, $\Delta H^{\neq}$ and $\Delta S^{\neq}$, were determined from rate constants values, k_{chem}, as described elsewhere (Quesada-Soriano *et al*., 2008).

Cloning, expression and purification

The double mutant C47S/Y108V was produced using a Quick Change TM Site-Direct Mutagenesis Kit (Stratagene). The double mutant was generated in two steps: first the single mutant C47S

was produced, using the expression plasmid pGST-1 (Battistoni *et al*., 1995) for site-directed mutagenesis. The PCR primers were:

47Ser/fw 5′-GGCTCACTCAAAGCCTCCTCCCTATACGGGCAGCTC CCC-3′

47Ser/rw 5′-GGGGAGCTGCCCGTATAGGGAGGAGGCTTTGAGTG AGCC-3′

The second site-directed mutation (Y108V) was produced using the plasmid pGST-1C47S as template. The PCR primers were:

108Val/fw 5′-CATCTCCCTCATCGTCACCAACTATGAGG-3′

108Val/rw 5′-CCTCATAGTTGGTGACGATGAGGGAGATG-3′

The PCR conditions were: 50 ng of DNA template, 125 ng each of forward and reverse primers, 10X reaction buffer, 0.8 nM of dNTP mix, PfuTurbo DNA polymerase (2.5U/μl) in a final volume of 50 μl. After one cycle of denaturing (95°C for 30 s), 16 cycles of denaturing (95°C for 30 s), annealing (55°C for 1 min) and extension (68°C for 5 min) were performed. Following temperature cycling, the product was treated with Dpn I restriction enzyme (10 U/μl) to digest the DNA template and to select for mutation-containing synthesized DNA. The double mutated plasmid was transformed into *E. coli* XL1-Blue supercompetent cells, and then was extracted using Nucleospin Plasmid (Macherey-Nagel GmbH & Co., Germany). The double mutant plasmid was once again transformed in *E. coli* TOP10 competent cells. These cells were grown in LB medium containing 100 μg/ml ampicillin and 50 μg/ml streptomycin. The synthesis of the enzyme was induced by addition of 0.5 mM isopropyl 1-thio-β-galactopyranoside (IPTG) when the absorbance at 600 nm was 0.5. Eighteen hours after induction, cells were harvested by centrifugation and lysed by ultrasonication. C47S/Y108V was purified by affinity chromatography on immobilized GSH (Simons and Vander Jagt, 1977). After affinity purification, the C47S/Y108V mutant enzyme was homogeneous as judged by SDS-PAGE. Then protein concentration was determined by the method of Lowry *et al.* (1951).

Kinetic studies

The enzymatic activities were determined spectrophotometrically at 25°C with different co-substrates (CDNB, EA, NBD-Cl) in a double-beam Cary 4000 spectrophotometer (Varian Instruments) equipped with a thermostated cuvette compartment under the conditions reported elsewhere (Lo Bello *et al*., 1997). Apparent kinetic parameters k_{cat}, $[S]_{0.5}$ and $k_{cat}/[S]_{0.5}$ for GSH using these co-substrates were determined at fixed concentrations of co-substrate and at different concentration of GSH, as reported elsewhere (Lo Bello *et al*., 1997). The cooperativity of the single C47S and the double C47S/Y108V mutant enzymes towards GSH were assayed by following the dependence of the enzymatic rate on GSH concentration (from 10 μM to 10 mM) at a constant CDNB concentration (1 mM) in 0.1 M potassium phosphate buffer (pH 6.5). Kinetic data were analysed by the KaleidaGraph (version 2.02, Abelbeck software) computer program and fitted to a rate equation expressing cooperativity as reported (Ricci *et al*., 1995). The best fit yielded the $[S]_{0.5}^{GSH}$ and Hill coefficient (n_H). Kinetic parameters reported in this paper represent the mean value of at least three experiments.

Fluorescence spectroscopy

Intrinsic fluorescence of wild-type (wt) and mutant GST P1-1 enzymes was measured with a Perkin Elmer LS50B spectrofluorometer equipped with a thermostatted sample holder set at 25°C. The experimental conditions and data analysis were similar to those described elsewhere (Téllez-Sanz *et al*., 2006; Quesada-Soriano *et al*., 2009). The binding of active site ligands to the C47S/Y108V GST P1-1 mutant quenches the intrinsic fluorescence of the enzyme as was described for wt GST P1-1 (Ricci *et al*., 1995; Ortiz-Salmerón *et al*., 2003; Caccuri *et al*., 1991). Equilibrium unfolding/refolding experiments were performed as described (Aceto *et al*., 1992) at 25°C in 20 mM sodium phosphate buffer, pH 7, containing 0.1 mM EDTA and 1 mM DTT.

Isothermal titration calorimetry (ITC)

Calorimetric experiments were conducted in an ultrasensitivity VP-ITC instrument (MicroCal Inc., Northampton, MA). The sample preparation and ITC experiments were carried out as previously described elsewhere (Téllez-Sanz *et al*., 2006; Quesada-Soriano *et al*., 2009). Titrations were routinely performed in 20 mM sodium phosphate, 5 mM NaCl, 0.1 mM EDTA at pH 7. Phosphate buffer was chosen because it is known to have a small enthalpy of ionization with only a slight pK_a change with rising temperature. Therefore, the observed enthalpy change, ΔH_{obs}, is the binding enthalpy change, ΔH_b, and consequently the heat contribution originating from possible protonation/deprotonation effects, associated with the binding process, can be assumed negligible. Blank titrations of ligand into buffer were also performed to correct for heat generated by dilution and mixing. Two models have been used to fit the experimental data: an equal and independent sites model (non-cooperative model) and a two equal and interacting sites model (cooperative model). The experimental data were fitted using 'Scientist' software (Micromath Scientific Software, St. Louis, USA) to the model algorithm implemented by us. The equations used in these models have been widely described in literature (Wyman and Gill, 1990). Finally, changes in the standard free energy ΔG^0 and entropy ΔS^0 were determined as $\Delta G^0 = -RT \cdot \ln K$ and $T\Delta S^0 = \Delta H - \Delta G^0$ (under the assumption that $\Delta H = \Delta H^0$).

Thermal stability

The thermal stability of the C47S/Y108V double mutant was examined in both activity assays and by differential scanning calorimetry (DSC). Different samples of the enzyme, at concentration of 0.1 mg/ml in 0.1 M phosphate buffer (pH 7.0) (containing 0.1 mM EDTA), were incubated at temperatures ranging 10–55°C for at least 15 min. At regular time intervals, aliquots were withdrawn from the incubation mixture and assayed for GST activity in the presence of 5 mM GSH and 1 mM CDNB.

DSC measurements were carried out on a VP-DSC ultrasensitive differential scanning calorimeter (Microcal Inc., Northampton). Prior to the DSC experiments, all samples were dialysed twice for several hours against 10 mM HEPES-NaOH at pH 7.5. Other experimental conditions were analogous to those described previously elsewhere (Quesada-Soriano *et al*., 2009). The DSC traces in the presence of EASG were recorded at least three times at each EASG concentration. The heating rate was routinely 1.5 K/min unless otherwise indicated. Reversibility of the thermal transitions was further checked by reheating the samples after fast cooling from the previous protein solution scan. Since thermal transitions were always found to be completely

irreversible, the calorimetric traces were baseline-corrected by subtracting the sample reheating scans.

The integration of the transition enthalpies, ΔH^{cal}, was carried out numerically and the van't Hoff enthalpies, ΔH^{VH}, were calculated according to

$$\Delta H^{VH}(T_m) = 4RT_m^2 \cdot \frac{C_P(T_m)}{\Delta H^{cal}(T_m)} \quad (1)$$

where T_m represents the temperature at maximal C_p of the unfolding reaction, and $C_p(T_m)$ and $\Delta H^{cal}(T_m)$ are the molar excess heat capacity and transition enthalpy, respectively, at T_m.

Crystallization

The apo C47S/Y108V GST P1-1 protein crystals were grown by streak seeding a drop containing 7.5 mg/ml C47S/Y108V GST, 22% (w/v) PEG 8000, 100 mM MES pH 6.0, 350 mM Ca acetate and 10 mM DTT with a cat's whisker that had been passed through a drop containing C47S/Y108V GST EASG complex crystals, grown as detailed below. Crystals grew over 2–3 days at 291 K. Attempts to co-crystallize the enzyme with EA or to soak in EA to existing apo crystals were unsuccessful. In the latter approach the resulting crystals displayed poor diffraction (smearing of diffraction spots) suggesting that the crystal lattice was being disrupted through binding of EA at, or close to, lattice interactions or that EA was causing conformational changes leading to disruption of the crystal lattice and degradation of the crystal quality. We note that neither wt nor the single mutant Y108V behaved in a similar fashion elsewhere (Oakley *et al*., 1997a; Quesada-Soriano *et al*., 2009).

In the case of the EASG enzyme complex, the protein, at 4 mg/ml, was pre-incubated with 5 mM EASG and 5 mM DTT for 24 h prior to crystallization. The protein complex was subsequently screened in an 8 × 96 well sparse matrix screen (the 'C3' screen) using sitting drop plates (SD-2, Innovadyne) at the Collaborative Crystallisation Centre (www.csiro.au/c3) with drops consisting of 200 nl protein and 200 nl reservoir. The plates were incubated at 20°C and were imaged 13 times over the course of 2 months. Of the 800 or so conditions trialled, crystals were observed in only one condition: 200 mM calcium acetate, 100 mM MES pH 6.0, 20% (w/v) PEG 8000 and 5 mM DTT. This condition was used to generate an optimized in-house screen using a scaled up 24 well plate format without any success. A 96 well grid was then generated using the following conditions: 200–400 mM calcium acetate, 16–24% (w/v) PEG 8K, 100 mM MES pH 6.0 and 5 mM DTT at 20°C. Many conditions yielded crystals which reached a suitable size in approximately 2 days. Data were collected from a crystal grown in 267 mM calcium acetate, 100 mM MES pH 6.0, 20% (w/v) PEG 8000 and 5 mM DTT. Crystals also grew in the absence of DTT under the same conditions.

Structure determination of the apo C47S/Y108V GST P1-1

The X-ray diffraction data were collected at the Australian Synchrotron on beamline 3BM1 (PX1) using Blue-Ice software (McPhillips *et al*., 2002) and a Quantum ADSC 210R detector at a wavelength of 0.957 Å. For cryoprotection the crystals were soaked for 2 min in the well solution containing 5% (v/v) MPD, then dipped briefly in well solution containing 10% (v/v) MPD. The crystals were then snap frozen at 100 K in the cryostream. The data were processed with XDS (Kabsch, 1993). The mutant protein crystallized in the usual GST P1-1 *C*2 spacegroup. The model was refined using REFMAC (Murshudov *et al*., 1997) with model building in COOT (Emsley and Cowtan, 2004). A round of rigid body refinement was performed using the Y108V EASG complex structure (in the same *C*2 spacegroup; PDB id: 3HJO), after removing all ligands, followed by a round of restrained positional refinement. The change of residue at position 47 was evident in the initial electron density maps, thus confirming the mutation at that position. Six calcium ions were identified binding to the dimer, two in positions normally observed for wt GST P1-1 and two additional calcium ions bound in the MES buffer binding site of each subunit as was also seen in the EASG complex of the single Y108V mutant elsewhere (Quesada-Soriano *et al*., 2009). The R_{cryst} and R_{free} for the final model were 17.1 and 21.0% respectively for all data to 1.8 Å resolution. A summary of the refinement statistics is given in Table 1. The model was analysed with the program PROCHECK (Laskowski *et al*., 1993) which showed that its stereochemical quality was similar or better than expected for structures refined at similar resolutions.

Structure determination of the C47S/Y108V EASG complex

Crystals of the complex grown in the absence of DTT were cryoprotected and frozen as described above. The X-ray diffraction data were collected using a R-AXIS IV++ area detector with CuK_α X-rays generated by a Rigaku MicroMax-007H rotating anode X-ray generator. The diffraction data were processed with MOSFLM (Leslie, 1992) and scaled with SCALA (Collaborative Computational Project, 1994). The model was built and refined as above. GSH and EA were built into the electron density maps and refined to occupancies of 100 and 70% respectively and have temperature factors of 21.7 and 29.7 $Å^2$ respectively. The R_{cryst} and R_{free} for the final model were 16.2 and 25.6%, respectively for all data to 2.6 Å resolution. A summary of the refinement statistics is given in Table 1. The model was analysed with the program PROCHECK (Laskowski *et al*., 1993) which showed that its stereochemical quality was similar or better than expected for structures refined at similar resolutions.

The X-ray diffraction data for the complex grown with DTT were collected using a R-AXIS IV++ area detector with CuK_α X-rays generated by a Rigaku MicroMax-007H rotating anode X-ray generator. The crystal was cryoprotected and frozen as described above. Diffraction data were processed with MOSFLM (Leslie, 1992) and scaled with SCALA (Collaborative Computational Project, 1994). This complex crystallized in the usual GST P1-1 *C*2 space group. The model was built and refined as described above. After several rounds of refinement, the electron density for the EASG ligand was evident in a $F_0 - F_c$ difference map and was subsequently built into the model. The GSH component refined with an occupancy of 100% in both subunits of the dimer while the EA refined to 30% occupancy with an average temperature factor of 19.1 $Å^2$. This difference between the occupancies suggests that some of the EASG has broken down and the mutation at Y108 means the enzyme cannot catalyse the Michael addition between the EA and GSH. This is also evident in the electron density maps where there is no continuous density at normal contours levels between GSH and the EA. The B-factors for surrounding residues after refinement were similar to those of the bound ligands, with the average B-factor for EA of 19.1 $Å^2$ and GSH of 18.2 $Å^2$. There were also six calcium ions identified as described above. The R_{cryst} and R_{free} for the final model were 15.5 and 20.6% respectively for all data to

Table 1. Summary of data collection and structure refinement

	EASG	EASG (no DTT)	Apo
Data collection			
Temperature (K)	100	100	100
Space group	*C*2	*C*2	*C*2
Cell dimensions			
a (Å)	75.9	75.9	74.3
b (Å)	89.2	89.3	89.4
c (Å)	69.2	69.4	69.2
β (°)	89.9	90.1	90.0
GST monomers in asymmetric unit	2	2	2
Maximum resolution (Å)	2.1	2.6	1.8
No. of crystals	1	1	1
No. of observations	193246	55001	270682
No. of unique reflections	26463	13960	39445
Data completeness (%)	98.2 (98.2)	97.7 (97.7)	94.0 (83.0)
R_{merge}	11.9 (37.5)	13.2 (33.6)	6.7 (26.0)
I/σ	5.5 (1.8)	4.6 (1.8)	21.6 (6.2)
Multiplicity	7.3	3.9	6.9
Refinement			
Non-hydrogen atoms			
Protein	3262	3249	3272
EA	39	39	—
GSH	40	40	—
PO_4^{2-}	—	—	5
Ca^{2+}	6	6	6
CO_3^{2-}	—	—	5
Solvent (H_2O)	477	271	482
Resolution (Å)	2.1	2.6	1.8
R_{cryst}[a] (%)	15.5	16.2	17.1
R_{free}[b] (%)	20.6	25.6	21.0
Reflections used in R_{cryst}			
Number	25 145	13 266	39 585
rmsd's from ideal geometry			
Bonds (Å)	0.013	0.020	0.013
Angles (°)	1.3	1.9	1.4
Wilson B-factor	18.1	31.2	28.1
Mean *B* (protein) (Å^2)			
Main-chain	12.3	14.7	18.6
Side-chain	13.1	14.9	19.9
Mean *B* (solvent) (Å^2)	22.5	12.9	28.5
Mean *B* (GSH) (Å^2)	18.2	21.7	—
Mean *B* (EA) (Å^2)	19.1	29.7	—
Residues in most favoured regions of Ramachandran plot	94.4	93.3	93.6
Residues in disallowed regions of Ramachandran plot (%)	0	0	0

The values in parentheses are for the highest resolution bin. $R_{merge} = \Sigma hkl \Sigma i |I_i - <I>| / |<I>|$, where I_i is the intensity for the *i*th measurement of an equivalent reflection with indices *h*, *k*, *l*.
[a] $R_{cryst} = \Sigma ||F_{obs}| - |F_{calc}|| / \Sigma |F_{obs}|$, where F_{obs} and F_{calc} are the observed and calculated structure factor amplitudes respectively.
[b] R_{free} was calculated with 5% of the diffraction data that were selected randomly and not used throughout refinement.

2.1 Å resolution. A summary of the refinement statistics is given in Table 1. The model was analysed with the program PROCHECK (Laskowski *et al.*, 1993) which showed that its stereochemical quality was similar or better than expected for structures refined at similar resolutions.

Computational docking of EA

EA was computationally docked into the dimer interface of a high-resolution crystal structure of GST P1-1 (PDB code: 5GSS) using the program FRED (V2.2.5, www.eyesopen.com.au). The

Journal of Molecular Recognition

Table 2. Specific activities of GST P1-1 wt and the double mutant (C47S/Y108V) with selected substrates

	Substrate specific activity (μmol mg^{-1} min^{-1})		
Enzyme	CDNB	EA	NBD-Cl
GST P1-1	110 ± 10	1.70 ± 0.01	2.9 ± 0.2
C47S	43 ± 2	2.47 ± 0.03	3.77 ± 0.07
Y108V[a]	45 ± 5	0.018 ± 0.002	8.3 ± 0.09
C47S/Y108V	44 ± 0.7	0.13 ±0.01	7.1 ± 0.4

All specific activity values are mean ± SEM and are based on three replicates.
[b]Data published in Nuccetelli *et al.* (1998).

receptor binding site had a site box volume of 2130 Å, with an outer contour of 1354 Å and an inner contour of 75 Å. For the docking run, 3 Å was added to the box in each dimension. A constraint was added which forced EA to be at the appropriate distance to form a covalent bond with Cys-101. One thousand docking poses were created by FRED, with the top 100 poses optimized by the Chemgauss3 scoring function and the top 20 poses kept for further analysis. A combination of visual analysis and scoring functions was used to obtain the most likely binding orientation, with the same result obtained whether GSH was bound at the G-site or not.

RESULTS

Kinetic studies with C47S/Y108V mutant of GST P1-1

Mutations at both Cys-47 and Tyr-108 residues have produced a double mutant with altered specific activities. With CDNB as a co-substrate, the specific activity is about half of that reported for wt consistent with the results shown by the respective single mutant enzymes (Table 2). With EA, it is significantly lowered with respect to that of wt. This greater reduction in specific activity seems mostly due to the mutation of Tyr-108 into valine, since the Y108V single mutant shows a specific activity which is about a 100 times lower than that of wt (Table 2). Finally, with NBD-Cl as the co-substrate there is an increase of specific activity in comparison with that of wt which, as with EA, is due to effect of the Y108V mutation at H-site.

A more detailed analysis was carried out by investigating steady state kinetic parameters with the above co-substrates and the results are summarized in Table 3. With CDNB as co-substrate, the most dramatic changes are in the K_m values for GSH (1 ± 0.02) and for CDNB (6.67 ± 1.83) reflecting the altered values already found in the single mutants C47S (Nuccetelli *et al.*, 1998) or Y108V (Ricci *et al.*, 1995), respectively (Table 3). The value for k_{cat} differs slightly but the overall catalytic efficiency is reduced approximately nine times with respect to that of wt (Table 3). Therefore, both mutations affect the enzymatic properties of the wt enzyme in binding of GSH or CDNB. The mutation of Cys-47 into serine induced a positive cooperativity in the binding of GSH. The Hill coefficient was determined to be 1.25. This is a lower but still significant compared to the single mutant C47S (1.43) (Ricci *et al.*, 1995) (Table 3).

In the case of EA as co-substrate, there is an increased K_m^{cosub} and a 32-fold decrease in k_{cat} compared with wt. The decrease in k_{cat} is due to the effect Y108V mutation at the H-site, which has been shown previously to be involved in catalysis by stabilizing the transition state in the conjugation reaction (Lo Bello *et al.*, 1997). We have also determined the kinetic parameters of EA using the single mutant C47S. As expected, because this mutation affects the G-site and not the H-site, no significant changes were observed in the overall kinetic parameters with respect to those of wt (Table 3).

With NBD-Cl as co-substrate, the double mutant showed increased K_m values with respect to either GSH or NBD-Cl. The turnover number is also significantly increased. Overall, there is a marked decrease of catalytic efficiency (from 250 ± 12 to 22.22 ± 5.24 k_{cat}/K_m^{cosub}) (Table 3). The effect on the efficiency of both mutations seemed to be additive given the overall increase of K_m with either substrate is more than 30 times compared to wt. A three-fold increase in k_{cat} can be attributed to the Y108V mutation and more specifically to the loss of hydroxyl moiety of Tyr-108 as was reported previously (Lo Bello *et al.*, 1997).

Table 3. Steady-state kinetic parameters of wt and mutants towards selected substrates

Substrate	Enzyme	$[S]_{0.5}^{GSH}$ (mM)	K_m^{cosub} (mM)	k_{cat} (s^{-1})	k_{cat}/K_m^{cosub} (s^{-1} mM^{-1})
CDNB	GST P1-1	0.15 ± 0.03	1.2 ± 0.1	79 ± 3	66 ± 3
	C47S	1.2 ± 0.14	1.36 ± 0.32	38 ± 2	28 ± 2
	Y108V	0.069 ± 0.02	4.9 ± 0.7	60 ± 2	12.0 ± 2
	C47S/Y108V	1 ± 0.02	6.67 ± 1.83	32.13 ± 0.74	7.52 ± 1.71
EA	GST P1-1	0.18 ± 0.02	0.23 ± 0.02	3.2 ± 0.2	15 ± 2
	C47S	0.31 ± 0.05	0.097 ± 0.01	2.19 ± 0.03	22.58 ± 0.35
	Y108V	1.07 ± 0.3	0.16 ± 0.04	0.065 ± 0.02	0.4 ± 0.02
	C47S/Y108V	0.25 ± 0.05	1.31 ± 0.49	0.106 ± 0.008	0.092 ± 0.013
NBD-Cl	GST P1-1	0.016 ± 0.001	0.007 ± 0.001	1.2 ± 0.2	250 ± 12
	C47S	0.069 ± 0.007	0.041 ± 0.006	3.255 ± 0.025	79.46 ± 0.54
	Y108V	0.077 ± 0.03	0.10 ± 0.04	6.7 ± 2	67 ± 8
	C47S/Y108V	0.51 ± 0.04	0.26 ± 0.01	6.55 ± 0.48	22.22 ± 5.24

Values ± SEM were estimated by non-linear regression analysis of experimental data using Graph Pad Prism 4.0 software.

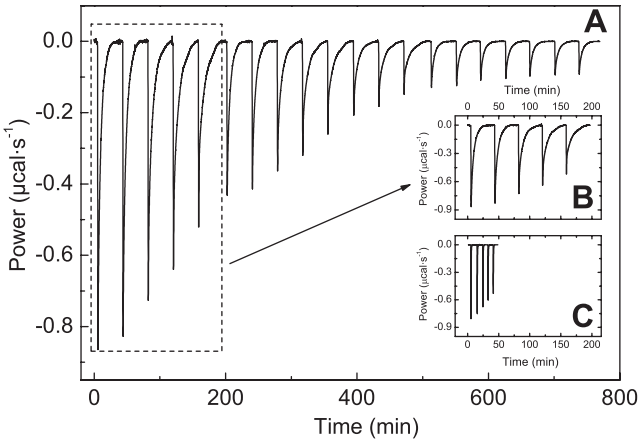

Figure 1. EA binding to C47S/Y108V. (A) Typical calorimetric thermogram for the titration of 70 μM C47S/Y108V mutant of GST P1-1 with 5 μl injections of 3.7 mM EA in 20 mM sodium phosphate, 5 mM NaCl and 0.1 mM EDTA at pH 7.0 and 35°C. (B) *Inset plot*: comparative plot between the first peaks from calorimetric thermogram shown in the main graph and some representative peaks from a calorimetric trace for a typical binding process in the absence of chemical processes (C).

Interaction of EA with C47S/Y108V mutant of GST P1-1

Figure 1 shows a typical experimental thermogram for the titration of the C47S/Y108V mutant with EA at pH 7.0 and 35°C. The negative values of calorimetric signals indicate an exothermic reaction. A potential chemical modification of the enzyme by EA binding to the double mutant is apparent from inspection of the calorimetric traces (Figure 1), and is similar to that detected for wt-enzyme and the Y108V single mutant (Quesada-Soriano *et al*., 2009). The baseline recovery (time response) after each injection of EA is very high (~30 min) compared to a typical binding process not involving a chemical reaction (~2 min) (Figure 1, inset). Thus, the calorimetric signal, corresponding to each EA injection, is composed of at least two exothermic heat contributions, *viz*., binding and chemical reaction. This behaviour was observed at all temperatures studied (16.2–42°C).

Since the highly reactive Cys-47, the main target of chemical modification by EA, is mutated to serine in this double mutant, it seems likely that the remaining reactive thiol residue, Cys-101, is the target for EA binding. This potential chemical reaction was undetected by fluorescence spectroscopy since the quenching curve appeared typical for a conventional non-covalent binding process. The kinetic (chemical reaction) and thermodynamic (binding) contributions were separated from the raw calorimetric data and analysed in analogous fashion to that described for the binding of EA to both wt-enzyme and Y108V mutant (Quesada-Soriano *et al*., 2009). The affinity of EA for the double mutant is similar to that deduced for the Y108V single mutant (Table 4). Moreover, the affinity found by fluorescence is in agreement with those deduced by ITC. The binding enthalpy change is small and negative at high temperatures, while at lower temperatures the enthalpy change is positive (unfavourable) (data not shown). Nevertheless, at all temperatures studied the entropy changes are always positive (favourable). The heat capacity change value, ΔC_p^0, calculated from a slope of a plot of ΔH_{obs} vs. temperature was negative (-0.20 ± 0.10 kcal mol K^{-1}) and similar to that deduced for the Y108V mutant (-0.25 ± 0.20 kcal mol^{-1} K^{-1}) (Quesada-Soriano *et al*., 2009). Thus, the additional point mutation, C47S, does not seem to affect the thermodynamic properties of ligand binding to the H-site of GST P1-1.

The kinetic constants, k_{chem}, at all temperatures studied, for the EA conjugation reaction, presumably with Cys-101, were lower than those determined for the Y108V mutant or wt enzyme (Table 5). An examination of the thermodependence of kinetic constants has allowed evaluation of both the activation energy and the thermodynamic activation parameters values for the conjugation reaction (Table 5).

Interaction of GSH, hexylSG and EASG with the C47S/Y108V mutant

The binding of GSH, EASG and hexylSG to the C47S/Y108V mutant was examined by ITC and fluorescence spectroscopy at several temperatures in the range of 15–38°C and pH 7.0. However, unlike the fluorescence intensities of the wt enzyme and single Y108V or C47S mutants, the fluorescence intensity of the C47S/Y108V double mutant increased by about 40% (using similar experimental conditions). Indeed, the double mutation seems to slightly alter the environment of the fluorophore/s responsible for protein fluorescence. This feature might be due to a small motion of Trp-38, located in the α2 loop and forming one wall of the G-site.

Figure 2 shows a typical ITC profile for the binding of EASG conjugate to the C47S/Y108V mutant, in phosphate buffer at pH 7.0 and 25.2°C. From the calorimetric profile it is clear that a non-cooperative model will not fit the data. Instead, a model of two equal and interacting sites can be fitted to all the calorimetric data irrespective of the temperature. Similar ITC experiments to those described for EASG were performed with the inhibitor

Table 4. Thermodynamic parameters for the binding of EA to GST P1-1 at 30.1°C and pH 7.0

Enzyme	$K \times 10^{-4}$ (M^{-1})	$-\Delta G^0$ (kcal mol^{-1})	$-\Delta H_{obs}$ (kcal mol^{-1})	$T\Delta S^0$ (kcal mol^{-1})	$-\Delta C_p$ (kcal mol^{-1} K^{-1})
wt[a,b]	4.5 ± 0.2	6.4 ± 0.6	5.3 ± 0.5	1.1 ± 0.1	0.38 ± 0.10
Y108V[a,b]	2.2 ± 0.3	6.0 ± 0.4	1.9 ± 0.2	4.1 ± 0.3	0.25 ± 0.13
C47S	1.2 ± 0.1	5.6 ± 0.4	6.2 ± 0.5	−0.6 ± 0.1	0.21 ± 0.04
C47S/Y108V[b]	3.2 ± 0.2	6.2 ± 0.3	1.4 ± 0.3	4.8 ± 0.6	0.20 ± 0.12
C47S/C101S	1.2 ± 0.2	5.7 ± 0.4	6.7 ± 0.4	−1.0 ± 0.2	0.23 ± 0.08

[a] Thermodynamic data determined in Quesada-Soriano *et al*. (2009).
[b] Thermodynamic data obtained by theoretical deconvolution of thermograms.

Journal of Molecular Recognition

Table 5. Kinetic and activation parameters in kcal/mol for EA conjugation reaction with wt-GST P1-1 and the Y108V and C47S/Y108V mutants a 30.1°C[a]

Parameter	C47S/Y108V	Y108V	wt
k_{chem}[b]	8.2×10^{-4}	3.1×10^{-3}	3×10^{-3}
E_a	20.1	4.6	1.8
ΔE_a	18.3	2.8	0
$\Delta G^{\neq}$	21.96	21.15	21.17
$\Delta\Delta G^{\neq}$	0.8	−0.02	0
$\Delta H^{\neq}$	19.5	4.0	1.2
$\Delta\Delta H^{\neq}$	18.3	2.8	0
$T\Delta S^{\neq}$	−2.5	−17.2	−20
$T\Delta\Delta S^{\neq}$	17.5	2.8	0

[a] $\Delta\Delta G^{\#}$, $\Delta\Delta H^{\#}$ and $T\Delta\Delta S^{\#}$ are the differences in each of the values from those obtained with wt-GST P1-1.
[b] k_{chem} is expressed as s^{-1}.

hexylSG. The binding of hexylSG to the C47S/Y108V mutant was also always cooperative in the temperature range studied. The observed enthalpy changes for both the 1st (ΔH_1) and the 2nd (ΔH_2) sites are negative in all cases. The binding equilibrium constant value for the second site is about 1.2 orders of magnitude higher than that for the first site in every case. An enthalpic-entropic compensation was deduced for both sites in the temperature range examined. A practically linear dependence was deduced for the global thermodynamic parameters (i.e. $\Delta H_g = \Delta H_1 + \Delta H_2$; $\Delta G_g^0 = \Delta G_1^0 + \Delta G_2^0$; $T\Delta S_g^0 = T(\Delta S_1^0 + \Delta S_2^0)$ (data not shown) for the three ligands (GSH, EASG and hexylSG). Moreover, the affinity for these ligands increases in the order GSH < hexylSG < EASG. Heat capacity change values obtained from the slope of ΔH_g vs. temperature were: $\Delta C_{p,g}^0 = -0.66 \pm 0.12$ kcal mol^{-1} K^{-1}; $\Delta C_{p,g}^0 = -1.24 \pm 0.31$ kcal mol^{-1} K^{-1}; $\Delta C_{p,g}^0 = -2.58 \pm 0.43$ kcal mol^{-1} K^{-1}, for GSH, hexylSG and EASG, respectively. The Hill coefficients, n_H, obtained from the calorimetric experiments did not change in the temperature range studied. However, an interesting correlation was obtained by inspection of the Hill coefficients for each ligand examined: (n_H (GSH): $1.35 < n_H$ (hexylSG): $1.42 < n_H$ (EASG): 1.47).

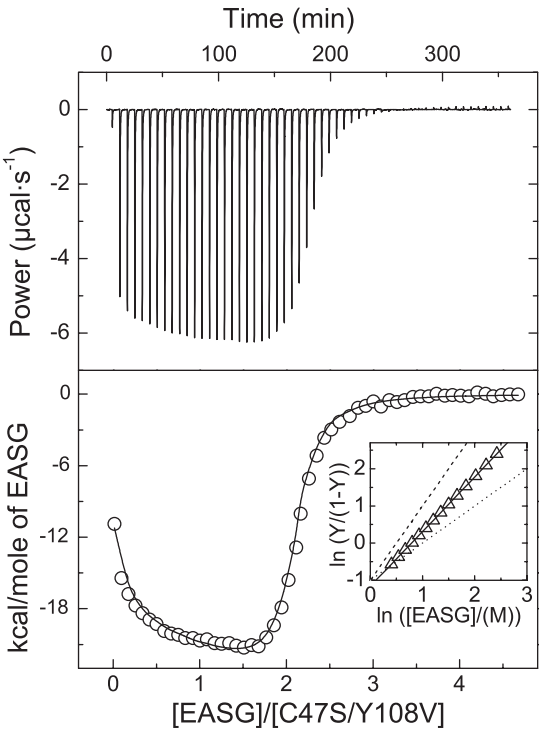

Figure 2. Representative isothermal titration calorimetry measurements of the cooperative binding of 1.56 mM EASG to 68 µM C47S/Y108V mutant of GST P1-1. Bottom panel shows the fit to a cooperative model with $K_1 = 1.1 \times 10^5$ M^{-1}, $K_2 = 1.3 \times 10^6$ M^{-1}, $\Delta H_1 = -11.0$ kcal/mol and $\Delta H_2 = -32.7$ kcal/mol. Titration was performed in 20 mM sodium phosphate, 5 mM NaCl and 0.1 mM EDTA at pH 7 and 25.2°C. *Inset plot*: Hill plot. The Hill coefficient value was 1.46 ± 0.03. Dashed and dotted lines represent the theoretical traces for $n_H = 2$ (infinite cooperativity) and $n_H = 1$ (no cooperativity), respectively.

Thermodynamic studies with C47S and C47S/C101S mutants

We carried out a thermodynamic study on the C47S and the C47S/C101S mutants using GSH, hexylSG, EA, EASG and EACys to explore the roles of these reactive cysteine residues in binding ligands.

Binding of EA and EACys

The binding of EA to the C47S mutant, at 25°C and pH 7.0, was non-cooperative with an affinity similar to that for the EACys conjugate and no covalent modification with EA was detected (Quesada-Soriano *et al*., 2009). Herein, we have further examined the thermodynamic properties at temperatures others than 25°C. The behaviour at temperatures ≤30°C, was consistent with typical binding values with a negative heat capacity value, i.e. the affinity slightly decreases and enthalpy changes become more favourable (more negative) as the temperature increases. However, at temperatures >35°C the calorimetric traces show an unexpected behaviour: the baseline recovery time after injection increases compared with typical binding (Figure 3A). This feature is more intensified in the first peaks (Figure 3A, inset). The experiments were repeated using either the same or other protein batches showing that the effect could be reproduced. In order to determine whether this effect, visualized at higher temperatures, was correlated with a potential conjugation of EA with some reactive group of the enzyme we carried out similar ITC experiments using the C47S mutant and the EACys conjugate under similar experimental conditions. The thermograms from these experiments did not display the abnormal features (data not shown), confirming that the differences observed in the first peaks of the ITC thermogram are intrinsically related to the chemical reaction of EA with a residue in the C47S mutant.

In the cysteine mutants, C47S and C47S/Y108V, the small effect detected in the calorimetric titration with EA, cannot be attributed to a chemical conjugation of the Cys-47 residue with EA. However, Cys-101 can also react with EA, albeit to a lesser extent than the Cys-47 residue. We would therefore expect similar results to be obtained for both C47S and C47S/Y108V mutants. Surprisingly however, the single C47S mutant does not display the effect at temperatures below 30°C. To investigate the involvement of Cys-101 in this process, we performed some calorimetric experiments with EA under the same experimental conditions with the double cysteine mutant, C47S/C101S. The

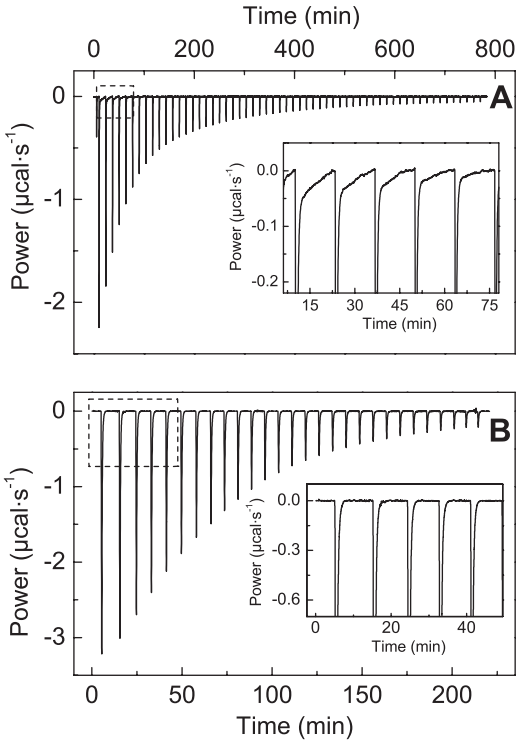

Figure 3. Representative isothermal titration calorimetry measurements of the binding of EA to both C47S (A) and C47S/C101S (B) mutants of GST P1-1 at 36 and 37°C, respectively. Titrations were performed in 20 mM sodium phosphate, 5 mM NaCl and 0.1 mM EDTA at pH 7.0. Zoom plots of the some peaks remarked are shown as *insets*. The chemical process (irreversible covalent modification of the enzyme with EA) is not apparent in the raw calorimetric data with the C47S/C101S mutant (panel B).

resultant calorimetric thermograms do not show any evidence (at temperatures between 15 and 42°C) that can be attributed to a chemical reaction, thus supporting Cys-101 as the site of interaction in the Cys-47 mutants (Figure 3B). The thermodynamic parameters obtained from the EA interaction with the C47S/C101S mutant were very similar to those found for the EA interaction with the C47S mutant (Table 4). Moreover, the C47S/C101S double mutant after titration with EA, could be recovered as the apo enzyme (by exhaustive dialysis without reducing agents) and used again in further ITC titration experiments demonstrating the non-covalent nature of EA binding in the double cysteine mutant. Further confirmation was found in the similar ITC thermograms for the C47S and C47S/C101S mutants.

Binding of GSH, hexylSG and EASG

The binding of GSH, hexylSG and EASG to the C47S and C47S/C101S mutants was cooperative under all the experimental conditions examined. This behaviour is very similar to that described above for the binding of these ligands to the C47S/Y108V double mutant. The main differences in the thermodynamic parameters deduced for the C47S/Y108V compared with those determined for the C47S and C47S/C101S mutants were found with the hexylSG and EASG inhibitors. However, GSH binding was similar for all three mutants (data not shown). The different behaviour found between hexylSG, EASG and GSH with the C47S/Y108V mutant compared with that for the C47S and C47S/C101S mutants can be attributed to the increase in hydrophobicity at the H-site as a consequence of the Y108 → V mutation given that the hexylSG and EASG inhibitor bind to both the H- and G-sites (Reinemer *et al*., 1992; Oakley *et al*., 1997a, b).

Thermal and chemical stability

The thermal stability of the C47S/Y108V mutant of GST P1-1 in the absence and in the presence of EASG was examined by DSC. In the absence of ligand, a single and irreversible transition was detected at all scan rates assayed. A clear dependence of T_m with the scan rate was observed, indicating a kinetic control, similar to that described previously for the Y108V mutant (Quesada-Soriano *et al*., 2009) and wt GST P1-1 (Ortiz-Salmerón *et al*., 2003) (Figure 4). However, the kinetic distortions due to an irreversible process seem to be negligible at high scan-rates and so the T_m (54.7°C) values reach a 'plateau' and the transition becomes more symmetric (Figure 4, inset). This behaviour resembles that described for the Y108V (T_m: 55.2°C) (Quesada-Soriano *et al*., 2009) and C47S single mutants (T_m: 56.1°C) (Téllez-Sanz *et al*., 2006) of GST P1-1. In this case, however, the theoretical plateau seems more clearly defined; thus there appears to be little or no scan-rate effect on the transition temperatures within the 1.15–1.5 K/min range, which supports that, for those scan-rates, kinetic distortions become negligible and the equilibrium thermodynamic analysis might be applicable (Vogl *et al*., 1997; Thórólfsson *et al*., 2002). The validity of this assumption can be also supported visualizing the symmetry of the endotherms at rate scans above 1.15 K/min. Furthermore, the van't Hoff enthalpy (Eq. 1) approaches the true calorimetric enthalpy at those heating rates, thereby yielding a cooperativity ratio $\Delta H^{cal}/\Delta H^{VH}$ close to unity. A similar thermal stability and unfolding pathway for the three mutants (C47S, Y108V and C47S/Y108V) can be deduced. Moreover, the thermal stability results observed from activity

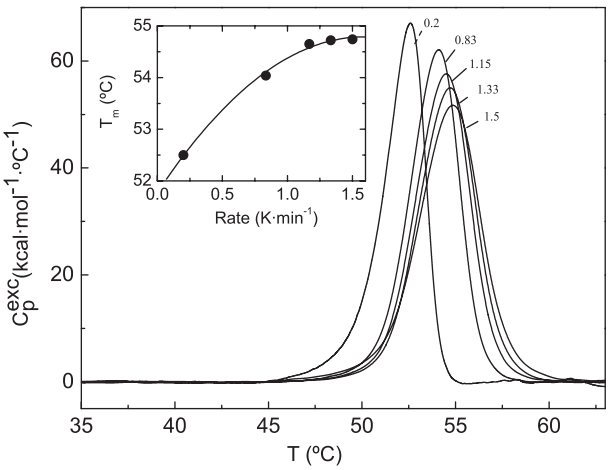

Figure 4. Variation with heating rate of the C_p transition curves of the C47S/Y108V mutant of GST P1-1. The number near to the peaks refers to the heating rates in Kelvin per minute. The buffer was 10 mM HEPES-NaOH at pH 7.5. The transition curves are normalized to zero initial heat capacity. The calorimetric enthalpy values determined were: 190.5, 209.6, 214.2, 212.0 and 220.6 kcal/mol (from lower to higher scan rate). The protein concentration in all calorimetric traces was 17.2 µM. Scan-rate effect on the transition temperatures (T_m) is displayed as inset. The continuous line has no theoretical meaning and is shown to guide the eye.

assays both for C47S/Y108V mutant and wt enzyme (data not shown), showed that the thermal stability was essentially unaffected by the double mutation.

Taken together, a non-two-state model could be adequate to describe the thermal unfolding mechanism for the C47S/Y108V mutant in the absence of ligand. The presence of different concentrations of the strong inhibitor EASG stabilizes the C47S/Y108V double mutant, analogously to wt and the Y108V mutant (Quesada-Soriano *et al*., 2009). Bimodal thermograms and a progressive increase in T_ms with ligand concentration are also observed (not shown). In addition, since the unfolding curves for the C47S/Y108V mutant, in the presence of EASG, were similar to those registered for the single Y108V mutant (Quesada-Soriano *et al*., 2009), the analysis of the traces was also identical.

Structural characterization

To complement the kinetic and thermodynamic data, we determined the crystal structures of the C47S/Y108V double mutant (apo form) and as EA and EASG complexes (Figure 5). No crystal structure was obtained for the EA C47S/Y108V complex due to the unwillingness of the complex to crystallize readily and the poor diffraction quality of the crystals when they did eventually grow. In contrast, the wt and the single Y108V mutant crystallize readily in the presence of EA (Oakley *et al*., 1997a; Quesada-Soriano *et al*., 2009).

We computationally docked EA into the dimer interface so that it forms a covalent bond with Cys-101 of one subunit and found the molecule packs such that it forms van der Waals contacts through its aromatic ring with Cys-101 of the other subunit, Ile-104 and Ser-105 as well as forming a salt bridge between its carboxylate and Arg-213 (Figure 6). In the wt enzyme, EA can also bind in the H-site in a non-productive manner (Oakley *et al*., 1997a). However, modelling suggests the interaction of EA with the H-site of the Y108V mutant would be much weaker due to the loss of the π-stacking interaction between EA and Y108.

The structures of the apo and EASG double mutant complex were readily solved. Neither structure differs significantly from the equivalent single mutant (Quesada-Soriano *et al*., 2009) or wt structures (Oakley *et al*., 1997a, b). The only differences of note are, firstly, at the site of the C47S mutation there is a small shift (alpha-carbon of residue 47 moves by 0.4 Å) compared to the single Y108V mutant and wt structures. In the double mutant (and single Y108V mutant) there is a water molecule missing near the ND2 atom of Asn-204 that normally forms a hydrogen bond with the Tyr-108 hydroxyl in the wt enzyme. Secondly, the α2 loop region appears well ordered in the apo structure in contrast to previously reported results with the wt enzyme (Oakley *et al*., 1998) where this region was not observed due to high mobility. The same region is also observed in the single mutant Y108V structure reported elsewhere (Quesada-Soriano *et al*., 2009). An explanation for the differences is that the mutants required a high concentration of calcium ions to crystallize and some of these ions form crystal contacts between the α2 loop region of one molecule with other protein molecules in the crystal lattice.

The EASG and apo structures are essentially identical with a few exceptions in the H-site binding pocket and in the water network at the dimer interface. There is a small, albeit significant, shift of several residues around the H-site, mainly residues contributing to the beginning of α2 loop including Val-35 and Gln-36, with the maximum movement in the alpha carbon atoms of approximately 0.7 Å (Figure 5B). Phe-8 has also shifted in the EASG compared to the apo structure in such a way that the phenyl ring has rotated by about 12° away from the ligand (Figure 5B). Overall, it appears that these movements have resulted in a widening of this site to accommodate the EA molecule.

The dimer interface of the EASG complex also differs somewhat from the apo structure in the position and number of water molecules. The Cys-101 side-chains also adopt different conformations. The different water structure in the apo structure is presumably a result of the absence of GSH and thus the usual connecting water network that runs through this interface. We cannot, however, rule out the possibility that the difference in the water network, with less waters in the dimer interface of the EASG complex, may be affected by some EA interaction (released from breakdown of EASG) with the Cys-101 residues although there is no evidence EA binding in the electron density in this region. Thus if EA has bound to Cys-101 it is very mobile.

Normally DTT is required for growing human GST P1-1 crystals but we were concerned that DTT would compete with EA for binding to the protein. Unfortunately, neither the apo protein or the EA complex could be crystallized in the absence of DTT suggesting the presence of EASG occupying the G- and H-sites was also important for growing the crystals in the absence of DTT. The structures of the EASG complex in the presence or absence of DTT are identical.

The structures of the EASG enzyme complex show that the aromatic ring of the EA moiety forms a π-stacking interaction with Phe-8 (Figure 5A) as observed previously for the single mutant Y108V complex (Quesada-Soriano *et al*., 2009). This is in contrast to the EASG wt structure in which the aromatic ring stacks between Tyr-108 and Phe-8 with predominant interactions with Tyr-108 (Oakley *et al*., 1997a).

DISCUSSION

In our previous work we studied the role of Tyr-108 in binding the diuretic drug EA but the analysis was complicated by covalent binding of EA to the very reactive cysteine residue, Cys-47 (Quesada-Soriano *et al*., 2009). Here we mutated Cys-47 to serine in order to overcome this problem. The EA interaction with the C47S/Y108V double mutant was studied by ITC and fluorescence spectroscopy. The affinity of EA to the double mutant was lower than that of the wt enzyme but very similar to that calculated for the Y108V single mutant (Table 4) (Quesada-Soriano *et al*., 2009). A chemical process was detected in the calorimetric thermograms, which can be associated with a covalent reaction of the ketone α,β-unsaturated of EA to some residue other than Cys-47. A two-step mechanism (binding and covalent reaction) can explain the interaction of EA with this double mutant as was the case for the Y108V single mutant (Quesada-Soriano *et al*., 2009). The binding of EA to double mutant is non-cooperative with a stoichiometry 1:1 (one molecule of EA per subunit of enzyme). The binding energy is favoured mainly by entropic contributions (Table 4). This behaviour is very similar to that described for the Y108V single mutant (Quesada-Soriano *et al*., 2009) although the enthalpy changes, ΔH_{obs}, are much smaller (less negative) (Table 4), consistent with a chemical process generating the broad calorimetric signals. Therefore, the conjugation reaction rate, deduced from the kinetic constant, is lower than that for the Y108V single mutant. In addition, the energetic barrier (activation

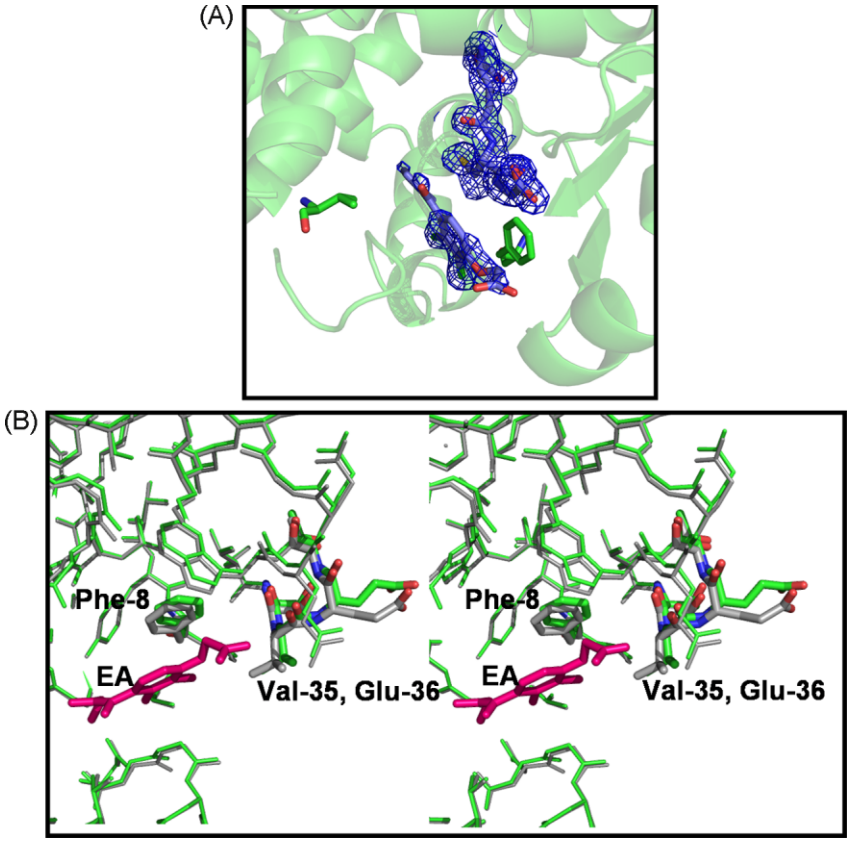

Figure 5. Structure of the EASG-Y108V/C47S mutant complex. (A) A close up view of the active site. The ligand is shown in blue bonds and the protein in green ribbon. Phe-8 and Val-108 are shown in green stick. The blue mesh shows the $2F_0 - F_c$ electron density map contoured at 1σ. (B) Stereoview of the H-site showing a superposition of the EASG complex on the apo structure of the same double mutant. EA is shown in purple bonds and the protein in green stick. Phe-8, Val-35 and Glu-36 are shown in thick green stick. The apo Y108V/C47S structure is shown as grey stick.

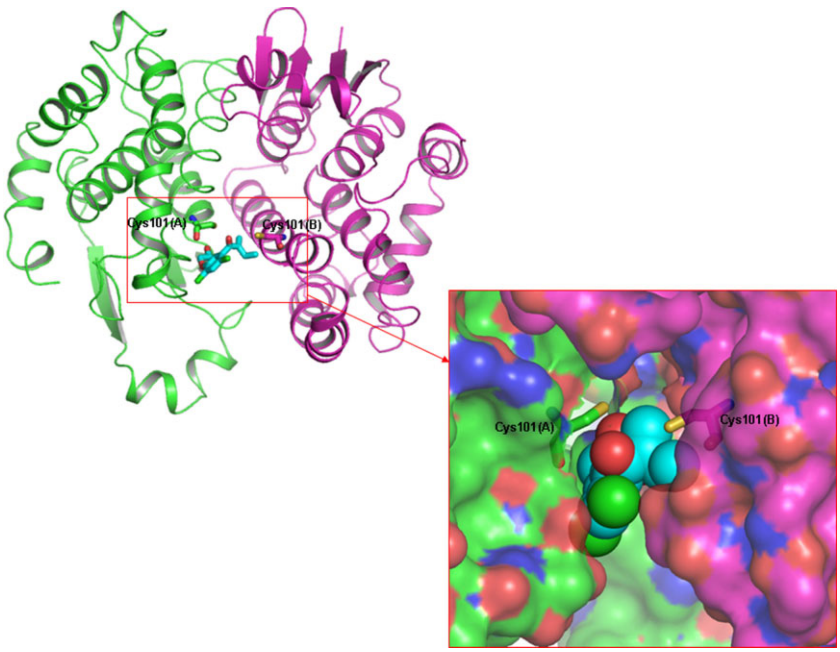

Figure 6. Computational docking of EA into the dimer interface of GST P1-1. Cartoon representation of Chain A (green) and Chain B (magenta) of GST (PDB code: 5GSS) with Cys101 highlighted as sticks from each chain. The docked solution of EA (cyan) is situated in the dimer interface. The addition of surface to both the GST molecule and the docked solution of EA, highlights that there is space for only one EA molecule to bind to Cys101 (highlighted as sticks) in the crystal structure.

Journal of Molecular Recognition

energy, E_a) for the double mutant, derived from an Arrhenius plot, is higher than that calculated for the Y108V mutant and wt-GST P1-1 (Table 5). According to transition state theory, analysis of the temperature dependence of a kinetic process allows for the determination of the activation parameters describing the differences between a ground state and the transition state of a reaction. The $\Delta\Delta G^{\#}$ parameter (Table 5) reflects the variation of kinetic constant, between the mutants and wt-enzyme. Moreover, $\Delta\Delta H^{\#}$, represents the variation of E_a, which is the main experimental parameter (i.e. $\Delta\Delta H^{\#} = \Delta E_a$). Given the lower activation enthalpy observed for wt-enzyme, the conjugation reaction rate would be enormous if the activation entropy is kept constant. A decrease of approximately 18 kcal/mol for E_a for wt enzyme (Table 5) increases the conjugation reaction rate by about 3.5-fold at 30°C. This is a consequence of the antagonistic effect of $\Delta\Delta S^{\#}$ arising from an unavoidable enthalpic-entropic compensation effect. As mentioned above, the wt enzyme displays a lower activation enthalpy that notably increases the conjugation reaction rate. This decrease in activation energy might be structurally achieved by a decrease in the number of enthalpy-driven interactions that have to be broken during the activation. Moreover, the structure of the activated state for the C47S/Y108V mutant:EA complex should adopt a conformation more flexible (higher entropy) than those for the Y108V/EA and wt/EA complexes (Table 5). The crystal structures of both apo Y108V (Quesada-Soriano *et al*., 2009) and apo C47S/Y108V mutants show an ordered α2 loop which appears to be an artefact of calcium-mediated crystal lattice contacts. Previous crystal structures of wt apo from crystals grown in the absence of calcium ions have revealed that the loop is highly mobile (Oakley *et al*., 1998). Additionally, the X-ray structures of an enzyme represents the average of the atomic positions, but atoms and portions of the enzyme often exhibit motions of sizable amplitudes about these averages, phenomena which is more pronounced in solution. One source of flexibility might be due to the Cys-47 → Ser point mutation, leading to a higher mobility of the α2 loop and structural communication between subunits (Lo Bello *et al*., 1993; Ricci *et al*., 1995) resulting in the observed cooperativity (Tyr-49 at the end of the α2 loop forms a 'ball-and-socket' interaction with the other subunit). Our structural observations and docking studies suggest that this increase of flexibility in C47S/Y108V:EA complex is a result of EA binding to Cys-101, leading to increased mobility at the dimer interface (see below).

Our kinetic results suggested the existence of another reactive group, less reactive than the Cys-47 residue, that is also susceptible to modification by EA binding and thus, responsible for the chemical process detected here. Among the four cysteine residues per subunit of GST P1-1, the Cys-47 and Cys-101 have shown to be the most reactive toward electrophilic compounds (Ricci *et al*., 1991; Lo Bello *et al*., 1995, 2001; Ang *et al*., 2007) whereas the remaining two cysteine residues are buried in the core of the molecule (Reinemer *et al*., 1992). Modification of the two most reactive cysteine residues interferes with the catalytic activity of GST P1-1 (Lo Bello *et al*., 1990; Tamai *et al*., 1990, 1991; Nishihira *et al*., 1992; Caccuri *et al*., 1992; Van Iersel *et al*., 1997; Hegazy *et al*., 2008). Mutation of Cys-47, the most reactive cysteine residue in GST P1-1 and the primary site for EA modification in the enzyme, leaves the remaining reactive cysteine, Cys-101 susceptible to attack. Thus, Cys-101 was hypothesized to be the target of EA covalent modification in the double mutant.

We have shown that both Cys-47 and Cys-101 are sites for covalent modification by EA and yet we have never seen the modification in crystal structures of EA complexes with wt or mutant enzymes. A possible reason is that our crystallization of human GST P1-1 normally requires DTT to be present and the reducing agent could inhibit EA reactivity with the enzyme. Despite extensive screening we were unable to produce crystals of the double mutant EA complex (or apo) in the absence of DTT. Attempts to soak EA solutions into preformed crystals resulted in poorly diffracting crystals consistent with EA binding at the dimer interface causing conformational changes leading to disruptions of the crystal lattice and thus disorder. Cys-101 is located, close to the neighbouring Cys-101 from the other subunit of the dimer. Modelling suggests there is only sufficient space at the dimer interface for one EA molecule unless conformational changes at the dimer interface are allowed. It is therefore possible that, in solution, the interface is flexible enough to bind EA molecules at both Cys-101 but in this case the interface would need to remain much wider then that seen in the crystal structures to accommodate both EA molecules simultaneously.

The binding of the inhibitors EASG and hexylSG to the double mutant shows a positive cooperativity. However, comparison of the apo enzyme structures of wt-enzyme and the C47S/Y108V mutant did not indicate any significant differences. Therefore, our results indicate that cooperativity was induced on binding of the ligands: i.e. the binding of EASG or hexylSG in the first subunit of the C47S/Y108V mutant induces a favourable conformational change on the second subunit, which then displays an increased affinity for the second molecule of either EASG or hexylSG. Analogous behaviour was observed in the binding of either GSH (Lo Bello *et al*., 1995; *in this work*) or GSNO (Téllez-Sanz *et al*., 2006) to the C47S single mutant. Studies reported in the literature (Lo Bello *et al*., 1993; Ricci *et al*., 1995) indicate the importance of the electrostatic interaction ($Cys\text{-}47^{-}/Lys\text{-}54^{+}$) for anchoring the flexible α2 loop and shaping the correct special arrangement for the binding of substrate in the active site. When this ion pair is disrupted, by mutation of either residue, the flexibility of this region could be greatly increased, causing α2 loop to contact the other subunit and generate a structural communication, which could be the basis for the observed positive cooperativity in the mutant C47S and the C47S/Y108V double mutant.

The ΔC_p^0 value obtained for GSH binding to the C47S/Y108V mutant (-0.66 kcal mol^{-1} K^{-1}) is very similar to that found for GSNO binding to the C47S single mutant ($\Delta C_p^0 = -0.58$ kcal mol^{-1} K^{-1}) (Téllez-Sanz *et al*., 2006). It is worth noting that the binding was cooperative in every case. However, this ΔC_p^0 value, contrasts with those determined previously for the binding of GSH: a higher and more negative value was determined for GSH binding to the double mutant compared with those calculated for wt (~ -0.29 kcal mol^{-1} K^{-1}) (Ortiz-Salmerón *et al*., 2003) or the Y108V single mutant (~ -0.21 kcal mol^{-1} K^{-1}) (Quesada-Soriano *et al*., 2009). In these cases, GSH binding was non-cooperative while in the C47S single mutant and the C47S/Y108V mutant, where the ionic pair $Cys\text{-}47^{-}/Lys\text{-}54^{+}$ is disrupted as a consequence of mutation, the GSH binding is cooperative. On the other hand, it is widely known that ΔC_p may be expressed in hydration terms ($\Delta C_p = 0.45\Delta ASA_{ap} - 0.26\Delta ASA_p$) where ΔASA_{ap} and ΔASA_p are the apolar and polar solvent-accessible surface area changes (before and after of binding), respectively (Spolar and Record, 1994; Gómez *et al*., 1995; Hilser *et al*., 1996). Moreover, a cooperative binding implies a conformational change and consequently the

solvent-accessible surface area changes will be higher. This observation would explain the ΔC_p values deduced for wt/GSH, (Ortiz-Salmerón *et al*., 2003) C47S/GSNO, (Téllez-Sanz *et al*., 2006) Y108V/GSH (Quesada-Soriano *et al*., 2009), and C47S/Y108V/GSH (in this work). In contrast, ΔC_p values for either hexylSG or EASG to the C47S/Y108V double mutant were higher and more negative than those calculated for GSH binding. It is important to emphasize that hexylSG and EASG inhibitors bind to both the G- and H-sites (Reinemer *et al*., 1992; Oakley *et al*., 1997a, b). When this occurs solvent-accessible surface area changes would be higher than those for GSH binding, and as such explains the ΔC_p values obtained. The higher and negative ΔC_p value for EASG compared to hexylSG can be explained by comparing the size and/or hydration volume of the hexyl and EA groups.

Analysis of the Hill coefficients reveals that the cooperativity increases (similarly to ΔC_p values) as the size and/or volume of the ligand increases. A similar behaviour was obtained by steady-state kinetics and fluorimetric experiments, for the C47S mutant with GSH (Ricci *et al*., 1995). The effect on cooperativity in the C47S/Y108V mutant seems entirely due the mutation Cys47 → Ser in the α2 loop which forms one wall of the G-site whereas the mutation Tyr108 → Val does not seem to have any effect. We can extend this finding to understanding the non-cooperative behaviour observed for binding of EA to H-site of the enzyme.

The small chemical effect, detected by ITC, upon EA binding to the C47S mutant at high temperatures might be a consequence of higher mobility of the α2 loop as the temperature increases. A similar dependence of the reactivity of the Cys-47 residue with temperature was also found for the GSNO interaction (Téllez-Sanz *et al*., 2006). It is puzzling that the kinetic effect observed for the C47S/Y108V double mutant, at all temperatures studied, is not observed in the C47S mutant at low temperatures. A possible explanation is that the binding energy (ΔH) of EA to the C47S mutant is large (much larger than binding energy of EA to the C47S/Y108V mutant) (Table 4) and consequently the heat due to the chemical effect (generated from the conjugation of Cys-101 with EA) is too small to be detected by ITC thermograms at low temperatures. However, as the temperature increases, the heat due to the chemical process increases, and consequently, this kinetic effect can be observed in the ITC traces.

Finally, the double substitution of Cys-47 and Tyr-108 with serine and valine, respectively, scarcely affected the thermostability of the enzyme. Remaining activities after 15 min incubation at various temperatures showed that the midpoint of the temperature-stability curve was 53°C for double mutant and 54°C for the wt enzyme. These results were very similar to those found by DSC. Two sequential and non-two-state transitions can describe phenomenologically the thermal unfolding pattern for this double mutant in the presence of EASG arisen from DSC studies. An analogous unfolding and dissociation pathway to those described for the Y108V mutant in the presence of EASG (Quesada-Soriano *et al*., 2009), can be used to represent the thermal unfolding for the C47S/Y108V mutant in the presence of EASG inhibitor. On the other hand, the urea-induced unfolding transition for the C47S/Y108V double mutant, and the resulting stability parameters, resembles those observed for wt and the single Y108V mutant (data not shown). The similar thermodynamic stabilities observed for the wt and mutant proteins are consistent with a negligible mutation-induced change in the core structure of the protein.

Concluding remarks

In summary, the additional Cys-47 → Ser point mutation to the Y108V mutant does not substantially alter the thermal or chemical stability nor the unfolding mechanism of GST P1-1 in either the absence or presence of ligand. It does, however, confirm that the Cys-101 residue is a target site for reaction with ligands if the primary thiol reactive residue, Cys-47, is unavailable. The dimer interface, and in particular Cys-101, has recently been identified as an important site for the binding of a range of anti-cancer drugs and may be a source of anti-cancer drug resistance by sequestering drugs before they reach the nucleus (Ang *et al*., 2009). Thus, the reactivity of the Cys-101 residue may be of great interest and importance. However, further studies are needed to explore the role of this residue as potential binding site of EA.

PROTEIN DATA BANK ACCESSION NUMBERS

The coordinates for the structures of the C47S/Y108V apo and EASG complexes, with and without DTT, are deposited in the Protein Databank (http://rcsb.org/pdb/) with the entry codes 3KMN, 3KM6 and 3KMO, respectively.

Acknowledgements

This work was supported in part by grant FQM 3141, Junta de Andalucía (Spain). This work was also supported by grants from the Australian Research Council (ARC) and the Australian Cancer Research Foundation to MWP. MLB was partially supported by MIUR-Italy (COFIN 2008). This research was undertaken on the PX1 beamline at the Australian Synchrotron, Victoria, Australia. The views expressed herein are those of the authors and are not necessarily those of the owner or operator of the Australian Synchrotron. The authors thank Dr Julian Adams and the other PX1 beamline staff for their assistance at the beamline. They also thank David Ascher for his help with mass spectrometry. Lorien Parker was supported by a National Health and Medical Research Council (NHMRC) Dora Lush Scholarship and an International Centre for Diffraction Data Crystallography Scholarship. M.W.P. is an ARC Federation Fellow and an NHMRC Honorary Fellow. I. Quesada-Soriano was the recipient of a fellowship from the Ministerio de Educación y Ciencia, Spain.

REFERENCES

Aceto A, Caccuri AM, Sacchetta P, Bucciarelli T, Dragani B, Rosato N, Federici G, Di Ilio C. 1992. Dissociation and unfolding of Pi-class glutathione transferase. Evidence for a monomeric inactive intermediate. *Biochem. J.* **285**: 241–245.

Ang WH, De Luca A, Chapuis-Bernasconi C, Juillerat-Jeanneret L, Lo Bello M, Dyson PJ. 2007. Organometallic ruthenium inhibitors of glutathione-S-transferase P1-1 as anticancer drugs. *ChemMedChem* **2**: 1799–1806.

Ang WH, Parker LJ, De Luca A, Juillerat-Jeanneret L, Morton CJ, Lo Bello M, Parker MW, Dyson PJ. 2009. Rational design of an organometallic glutathione transferase inhibitor. *Angew. Chem. Int. Ed. Engl.* **48**: 3854–3857.

Awasthi S, Srivastava SK, Ahmad F, Ahmad H, Ansari GA. 1993. Interactions of glutathione S-transferase-pi with ethacrynic acid and its glutathione conjugate. *Biochim. Biophys. Acta* **1164**: 173–178.

Battistoni A, Mazzetti AP, Petruzzelli R, Muramatsu M, Federici G, Ricci G, Lo Bello M. 1995. Cytoplasmic and periplasmic production of human placental glutathione transferase in *Escherichia coli*. *Protein Expr. Purif.* **6**: 579–587.

Black SM, Beggs JD, Hayes JD, Bartoszek A, Muramatsu M, Sakai M, Wolf CR. 1990. Expression of human glutathione S-transferases in *Saccharomyces cerevisiae* confers resistance to the anticancer drugs adriamycin and chlorambucil. *Biochem. J.* **268**: 309–315.

Caccuri AM, Aceto A, Rosato N, Di Ilio C, Piemonte F, Federici G. 1991. Intrinsic fluorescence quenching of glutathione transferase pi by glutathione binding. *Ital. J. Biochem.* **40**: 304–311.

Caccuri AM, Petruzzelli R, Polizio F, Federici G, Desideri A. 1992. Inhibition of glutathione transferase pi from human placenta by 1-chloro-2,4-dinitrobenzene occurs because of covalent reaction with cysteine 47. *Arch. Biochem. Biophys.* **297**: 119–122.

Collaborative Computational Project, Number 4. 1994. The CCP4 suite: programs for protein crystallograhy. *Acta Crystallogr. D Biol. Crystallogr.* **50**: 760–763.

Emsley P, Cowtan K. 2004. Coot: model-building tools for molecular graphics. *Acta Crystallogr. D Biol. Crystallogr.* **60**: 2126–2132.

Fersht AR. 1999. Structure and Mechanism in Protein Science: A Guide to Enzyme Catalysis and Protein Folding. Freeman WH: New York.

Gómez J, Hilser VJ, Xie D, Freire E. 1995. The heat capacity of proteins. *Proteins* **22**: 404–412.

Hatayama I, Satoh K, Sato K. 1990. A cDNA sequence coding a class pi glutathione S-transferase of mouse. *Nucl. Acids Res.* **18**: 4606.

Hayes JD, Flanagan JU, Jowsey IR. 2005. Glutathione transferases. *Annu. Rev. Pharmacol. Toxicol.* **45**: 51–88.

Hegazy UM, Tars K, Hellman U, Mannervik B. 2008. Modulating catalytic activity by unnatural amino acid residues in a GSH-binding loop of GS P1-1. *J. Mol. Biol.* **376**: 811–826.

Hilser VJ, Gómez J, Freire E. 1996. The enthalpy change in protein folding and binding: refinement of parameters for structure-based calculations. *Proteins* **26**: 123–133.

Kabsch W. 1993. Automatic processing of rotation diffraction data from crystals of initially unknown symmetry and cell constants. *J. Appl. Cryst.* **26**: 795–800.

Kim KE, Onesti G, Moyer JH, Swartz C. 1971. Ethacrynic acid and furosemide. Diuretic and hemodynamic effects and clinical uses. *Am. J. Cardiol.* **27**: 407–415.

Laskowski RA, MacArthur MW, Moss DS, Thornton JM. 1993. PROCHECK: a program to check the stereochemical quality of protein structures. *J. Appl. Cryst.* **26**: 283–291.

Leslie AGW. 1992. Recent changes to the MOSFLM package for processing film and image plate data. *Joint CCP4+ ESF-EAMCB Newsletter on Protein Crystallography 26.*

Lo HW, Ali-Osman F. 2007. Genetic polymorphism and function of glutathione S-transferases in tumor drug resistance. *Curr. Opin. Pharmacol.* **7**: 367–374.

Lo Bello M, Battistoni A, Mazzetti AP, Board PG, Muramatsu M, Federici G, Ricci G. 1995. Site-directed mutagenesis of human glutathione transferase P1-1 Spectral, kinetic and structural properties of Cys-47 and Lys-54 mutants. *J. Biol. Chem.* **270**: 1249–1253.

Lo Bello M, Nuccetelli M, Caccuri AM, Stella L, Parker MW, Rossjohn J, McKinstry WJ, Mozzi AF, Federici G, Polizio F, Pedersen JZ, Ricci G. 2001. Human glutathione transferase P1-1 and nitric oxide carriers; a new role for an old enzyme. *J. Biol. Chem.* **276**: 42138–42145.

Lo Bello M, Oakley AJ, Battistoni A, Mazzetti AP, Nuccetelli M, Mazzarese G, Rossjohn J, Parker MW, Ricci G. 1997. Multifunctional role of Tyr 108 in the catalytic mechanism of human glutathione transferase P1-1 Crystallographic and kinetic studies on the Y108F mutant enzyme. *Biochemistry* **36**: 6207–6217.

Lo Bello M, Parker MW, Desideri A, Polticelli F, Falconi M, Del Boccio G, Pennelli A, Federici G, Ricci G. 1993. Peculiar spectroscopic and kinetic properties of Cys-47 in human placental glutathione transferase. Evidence for an atypical thiolate ion pair near the active site. *J. Biol. Chem.* **268**: 19033–19038.

Lo Bello M, Petruzzelli R, De Stefano E, Tenedini C, Barra D, Federici G. 1990. Identification of a highly reactive sulphydryl group in human placental glutathione transferase by a site-directed fluorescent reagent. *FEBS Lett.* **263**: 389–391.

Lowry OH, Rosebrough NJ, Farr AS, Randall RJ. 1951. Protein measurement with the Folin phenol reagent. *J. Biol. Chem.* **193**: 265–275.

Mannervik B, Board PG, Hayes JD, Listowsky I, Pearson WR. 2005. Nomenclature for mammalian soluble glutathione transferases. *Methods Enzymol.* **401**: 1–8.

McPhillips TM, McPhillips SE, Chiu HJ, Cohen AE, Deacon AM, Ellis PJ, Garman E, Gonzalez A, Sauter NK, Phizackerley RP, Soltis SM, Kuhn P. 2002. Blu-Ice and the Distributed Control System: software for data acquisition and instrument control at macromolecular crystallography beamlines. *J. Synchrotron. Rad.* **9**: 401–406.

Meyer DJ, Coles B, Pemble SE, Gilmore KS, Fraser GM, Ketterer B. 1991. Theta, a new class of glutathione transferases purified from rat and man. *Biochem. J.* **274**: 409–414.

Murshudov GN, Vagin AA, Dodson EJ. 1997. Refinement of macromolecular structures by the maximum-likelihood method. *Acta Crystallogr. D Biol. Crystallogr.* **53**: 240–255.

Nishihira T, Ishibashi T, Sakai M, Nishi S, Kumazaki T, Hatanaka Y, Tsuda S, Hikichi K. 1992. Characterization of cysteine residues of glutathione S-transferase P: evidence for steric hindrance of substrate binding by a bulky adduct to cysteine 47. *Biochim. Biophys. Res. Commun.* **188**: 424–432.

Nuccetelli M, Mazzetti AP, Rossjohn J, Parker MW, Board P, Caccuri AM, Federici G, Ricci G, Lo Bello M. 1998. Shifting substrate specificity of human glutathione transferase (from class Pi to class alpha) by a single point mutation. *Biochem. Biophys. Res. Commun.* **252**: 184–189.

Oakley AJ, Lo Bello M, Mazzetti AP, Federici G, Parker MW. 1997. The glutathione conjugate of ethacrynic acid can bind to human pi class glutathione transferase P1-1 in two different modes. *FEBS Lett.* **419**: 32–36.

Oakley AJ, Lo Bello M, Ricci G, Federici G, Parker MW. 1998. Evidence for an induced-fit mechanism operating in pi class glutathione transferases. *Biochemistry* **37**: 9912–9917.

Oakley AJ, Rossjohn J, Lo Bello M, Caccuri AM, Federici G, Parker MW. 1997. The three-dimensional structure of the human Pi class glutathione transferase P1-1 in complex with the inhibitor ethacrynic acid and its glutathione conjugate. *Biochemistry* **36**: 576–585.

Ortiz-Salmerón E, Nuccetelli M, Oakley AJ, Parker MW, Lo Bello M, García-Fuentes L. 2003. Thermodynamic description of the effect of the mutation Y49F on human glutathione transferase P1-1 in binding with glutathione and the inhibitor S-hexylglutathione. *J. Biol. Chem.* **278**: 46938–46948.

Phillips MF, Mantle TJ. 1991. The initial-rate kinetics of mouse glutathione S-transferase YfYf. Evidence for an allosteric site for ethacrynic acid. *Biochem. J.* **275**: 703–709.

Ploemen JH, van Ommen B, van Bladeren PJ. 1990. Inhibition of rat and human glutathione S-transferase isoenzymes by ethacrynic acid and its glutathione conjugate. *Biochem. Pharmacol.* **40**: 1631–1635.

Ploemen JH, Van Schanke A, Van Ommen B, Van Bladeren PJ. 1994. Reversible conjugation of ethacrynic acid with glutathione and human glutathione S-transferase P1-1. *Cancer Res.* **54**: 915–919.

Quesada-Soriano I, Leal I, Casas-Solvas JM, Vargas-Berenguel A, Barón C, Ruiz-Pérez LM, González-Pacanoswka D, García-Fuentes L. 2008. Kinetic and thermodynamic characterization of dUTP hydrolisis by *Plasmodium falciparum* dUTPase. *Biochim. Biophys. Acta* **1784**: 1347–1355.

Quesada-Soriano I, Parker LJ, Primavera A, Casas-Solvas JM, Vargas-Berenguel A, Barón C, Morton CJ, Mazzetti AP, Lo Bello M, Parker MW, García-Fuentes L. 2009. Influence of the H-site residue 108 on human glutathione transferase P1-1 ligand binding: structure-thermodynamic relationships and thermal stability. *Protein Sci.* **18**: 2454–2470.

Reinemer P, Dirr HW, Ladenstein R, Huber R, Lo Bello M, Federici G, Parker MW. 1992. Three-dimensional structure of class pi glutathione S-transferase from human placenta in complex with S-hexylglutathione at 2.8Å resolution. *J. Mol. Biol.* **227**: 214–226.

Ricci G, Del Boccio G, Pennelli A, Lo Bello M, Petruzzelli R, Caccuri AM, Barra D, Federici G. 1991. Redox forms of human placenta glutathione transferase. *J. Biol. Chem.* **266**: 21409–21415.

Ricci G, Lo Bello M, Caccuri AM, Pastore A, Nuccetelli M, Parker MW, Federici G. 1995. Site-directed mutagenesis of human glutathione transferase P1-1. *J. Biol. Chem.* **270**: 1243–1248.

Simons PC, Vander Jagt DL. 1977. Purification of glutathione S-transferases from human liver by glutathione-affinity chromatography. *Anal. Biochem.* **82**: 334–341.

Spolar RS, Record MT. 1994. Coupling of local folding to site-specific binding of proteins to DNA. *Science* **263**: 777–784.

Tamai K, Satoh K, Tsuchida S, Hatayama I, Maki T, Sato K. 1990. Specific inactivation of glutathione S-transferases in class Pi by SH-modifiers. *Biochem. Biophys. Res. Commun.* **167**: 331–338.

Tamai K, Shen HX, Tsuchida S, Hatayama I, Satoh K, Yasui A, Oikawa A, Sato K. 1991. Role of cysteine residues in the activity of rat glutathione transferase P (7–7): elucidation by oligonucleotide site-directed mutagenesis. *Biochem. Biophys. Res. Commun.* **179**: 790–797.

Téllez-Sanz R, Cesareo E, Nuccetelli M, Aguilera AM, Barón C, Parker LJ, Adams JJ, Morton CJ, Lo Bello M, Parker MW, García-Fuentes L. 2006. Calorimetric and structural studies of the nitric oxide carrier S-nitrosoglutathione bound to human glutathione transferaseP1-1. *Protein Sci.* **15**: 1093–1105.

Thórólfsson M, Ibarra-Molero B, Fojan P, Petersen SB, Sanchez-Ruiz JM, Martínez A. 2002. L-phenylalanine binding and domain organization in human phenylalanine hydroxylase: a differential scanning calorimetry study. *Biochemistry* **41**: 7573–7585.

Townsend DM, Findlay VL, Tew KD. 2005. Glutathione S-transferases as regulators of kinase pathways and anticancer drug targets. *Methods Enzymol.* **401**: 287–307.

Tsuchida S, Sekine Y, Shineha R, Nishihira T, Sato K. 1989. Elevation of the placental glutathione S-transferase form (GST-pi) in tumor tissues and the levels in sera of patients with cancer. *Cancer Res.* **49**: 5225–5229.

Van Iersel ML, Ploemen JP, Lo Bello M, Federici G, van Bladeren PJ. 1997. Interactions of alpha, beta-unsaturated aldehydes and ketones with human glutathione S-transferase P1-1. *Chem. Biol. Interact.* **108**: 67-78.

Vega MC, Walsh SB, Mantle TJ, Coll M. 1998. The three-dimensional structure of Cys-47-modified mouse liver glutathione S-transferase P1-1 Carboxymethylation dramatically decreases the affinity for glutathione and is associated with a loss of electron density in the alphaB-310B region. *J. Biol. Chem.* **273**: 2844–2850.

Vogl T, Jatzke C, Hinz HJ, Benz J, Huber R. 1997. Thermodynamic stability of annexin V E17G: equilibrium parameters from an irreversible unfolding reaction. *Biochemistry* **36**: 1657–1668.

Wilce MC, Parker MW. 1994. Structure and function of glutathione S-transferases. *Biochim. Biophys. Acta* **1205**: 1–18.

Wyman J, Gill SJ. 1990. Binding and Linkage: Functional Chemistry of Biological Macromolecules. University Science Books: Mill Valley, California; 123–163.